The 7th International Supercritical CO_2 Power Cycles Symposium
February 21 – February 24, 2022, San Antonio, Texas

Paper #3

MEASUREMENT OF CONVECTIVE HEAT TRANSFER COEFFICIENTS WITH SUPERCRITICAL CO_2 IN NOVEL ADDITIVELY MANUFACTURED HELICALLY PATTERNED PIN FIN TUBES USING THE WILSON PLOT TECHNIQUE

Matthew Searle[1, 2], Jim Black[3], Doug Straub[2], Ed Robey[2, 4], Joe Yip[2], Sridharan Ramesh[2, 4], Arnab Roy[2, 4], Adrian S. Sabau[5], Fred List III[5], Keith Carver[5], Darren Mollot[6]

ABSTRACT

This paper describes the measurement of convective heat transfer coefficients and friction factors for sCO_2 flowing in pin-fin patterned pipes in the Heat Exchange and Experimental Testing (HEET) facility at the US DoE's National Energy Technology Laboratory (NETL) in Morgantown, WV. The measurement procedures in the HEET rig were validated by conducting benchmark tests with smooth stainless-steel tube and comparing the results with published correlations for Nusselt number (Nu) and friction factor. Over typical Reynolds number range in sCO_2, the measured Nu and friction factors were within 7% of classical correlations for smooth tube flow.

The candidate pin fin patterned pipes were additively manufactured (AM) at the Oak Ridge National Laboratory. The pins were circular or elliptical in cross-section. Pin length to diameter aspect ratios were 1.33 and 2, while the pin diameter to tube diameter ratio was 0.188 and 0.125. Tests were performed for Re_D varying from 6.9×10^4 to 2.2×10^5 and at conditions equivalent to the low pressure outlet (8.69 MPa, 361 K) of the low temperature recuperator (LTR) in an indirect sCO_2 power cycle. The Wilson plot technique was utilized to measure the bulk heat transfer coefficients.

For the better performing design (tube A, pin length to tube diameter ratio: 1.33, pin diameter to tube diameter ratio: 0.188), the local heat transfer coefficient increased by 112% relative to the Dittus-Boelter correlation at the LTR low pressure outlet. This corresponded to a 282% increase in the product of the heat transfer coefficient and the surface area. Large pressure drops across the test articles were observed.

---

[1] Presenter, NETL/ORISE Postdoctoral Researcher, 3610 Collins Ferry Rd, Morgantown, WV 26505, 1(304) 285-4735, matthew.searle@netl.doe.gov
[2] US Department of Energy, National Energy Technology Laboratory, Morgantown, WV
[3] US Department of Energy, National Energy Technology Laboratory, Pittsburgh, PA
[4] Leidos Research Support Team, Morgantown, WV
[5] Oak Ridge National Laboratory, Oak Ridge, TN
[6] US Department of Energy, Washington, DC

INTRODUCTION

Presently there is worldwide interest in sCO_2 power generation technology as it has the potential to offer a five percentage point increase in cycle efficiency and an order of magnitude decrease in turbomachinery volume relative to conventional steam Rankine cycles (The five percentage point increase in efficiency corresponds to an 11% increase from a steam Rankine cycle efficiency of 45% to an indirect sCO_2 recompression Brayton cycle efficiency of 50%, with both cycles operating at a turbine inlet temperature of 700 °C) [1]. Thermodynamic models for direct and indirect sCO_2 cycles have been considered. Both cycles are based on the recuperated Brayton cycle [2, 3]. The results of the present study consider heat transfer at conditions in the indirect Brayton cycle.

Both direct and indirect sCO_2 cycles require significant recuperation (3–4 times net plant output). Thus, cost-effective recuperators are required [4]. For a given heat exchanger manufacturing technology, the capital cost of the heat exchanger equipment scales with the material volume. The material volume may be reduced through strategies for enhancing heat transfer from the hot stream to the cold stream. One such strategy is the addition of internal heat transfer enhancement features which increase the heat transfer through greater internal surface area and larger heat transfer coefficients. This strategy is successful when the increase in heat transfer is sufficiently greater than the increase in pressure drop so that a shorter heat exchanger may be built, which transfers the same quantity of heat at the same pumping power while using less material volume.

Two heat exchanger technologies that are being considered for implementation in sCO_2 power cycles are 1) printed circuit heat exchangers (PCHE) and 2) conventional shell and tube heat exchangers [5]. PCHE have higher thermal performance than shell and tube heat exchangers. However, heat transfer enhancement features for shell and tube heat exchangers, which were previously challenging to manufacture by conventional processes, can now be manufactured by additive manufacturing. The present work considers a novel helical pin fin pattern to increase the heat transfer on the tube side of a shell and tube heat exchanger. The helical pattern enhances heat transfer by creating swirl flow, while the pinned pattern promotes mixing through vortex shedding. Additively manufactured enhanced heat transfer features in shell and tube heat exchangers may increase their thermal performance to be competitive with PCHE. Further, additive manufacture will allow fabrication of enhanced shell and tube heat exchangers in a single build. This has the potential to make shell and tube technology competitive with PCHE from a manufacturing standpoint.

The Wilson plot technique allows experimental measurement of heat transfer coefficients on the hot or cold side of a heat exchanger as opposed to the heat exchanger's overall resistance. This is invaluable when systematically determining the benefit of specific heat transfer enhancements. Wilson first introduced the technique for scenarios where there was a very high heat transfer coefficient (typical of boiling or condensation) on the reference side, the side opposite of the heat exchanger test side [6]. The Wilson plot technique has been modified to consider scenarios where the requirement of a large heat transfer coefficient on the reference side has been relaxed. In this scenario, the heat transfer coefficient of the test side is obtained by varying the flow rate of the test side while maintaining the thermal resistance on the reference side constant by controlling the reference side flow rate and average temperature [4, 7, 8]. In this study, we utilize the modified Wilson plot method to measure the heat transfer coefficient at the tube side of the test article.

EXPERIMENTAL FACILITY

The NETL Heat Exchange and Experimental Testing (HEET) facility at the U.S. DoE's National Energy Technology Laboratory is a closed loop, sCO_2 heat exchanger test rig [4]. In the present test, the facility was utilized to measure tube-side heat transfer coefficients in a sCO_2 single-pass, counter-flow, tube and shell heat exchanger. The inlets and outlets of the heat exchanger were instrumented so that the inlet and outlet temperatures were measured as well as the differential pressures and inlet gauge pressures.

Capabilities of the HEET test facility include pressure to 24 MPa (3,500 psig), temperature to 811 K (1,000°F), mass flow rate to 1.5 kg/s (3 lbm/s), and Re to 500,000. In its present state, the maximum operating temperature on the cold fluid side is limited to 477 K (400 °F) due to the maximum allowable temperature for the Coriolis flow meters and 671 K (750 °F) on the hot fluid side due to the maximum allowable tube temperature.

TEST ARTICLES

Five inner tube designs were considered: a conventional tube, a tube composed of welded segments (referred to as the "conventional welded tube"), a tube composed of finless AM tube segments, and two tubes composed of welded segments of fin designs A and B. All test articles were made of 316L stainless steel. The tubing had an inner diameter of 7 mm (0.275 inch) and a wall thickness of 1.2 mm (0.049 inch). The additively manufactured test articles were fabricated by direct laser metal sintering (DLMS) at the Oak Ridge National Laboratory.

The tube length was 127 mm (5 inches) due to limitations in the AM volume chamber. To create a test article, five tubes were joined by orbital welding. To verify that the welds did not influence the results, a conventional tube was cut into five segments and welded back together. The same set of tests as the smooth conventional tube were performed on this article, and the difference in Nusselt number ratio, Nu/Nu_0, was less than 10%. All heat exchanger lengths were 0.64 m (2.1 ft) except for the conventional tube which was 1.52 m (5 ft).

In Figure 1, CAD models of tubes A and B are displayed in panels (a) and (b), respectively. Note that these tubes are 4:7 scale reproductions of the experimental tubes and have shorter lengths. Parameters for the tube designs are shown in Table 1; for more details see Searle et al. [9]. Initially, eighteen tube designs, which spanned the range of parameters, were considered. The two tube designs (A, B) were selected based on engineering considerations since all the tubes could not be built and tested. In this table, new nomenclature is introduced. A and A_0 are the internal surface area for finned and finless tubes, respectively. We note that the pin helical spacing and the helix pitch are nondimensional. The pin helical spacing, s, is scaled by the pin major diameter and the helix pitch, p, is scaled by the tube inner diameter.

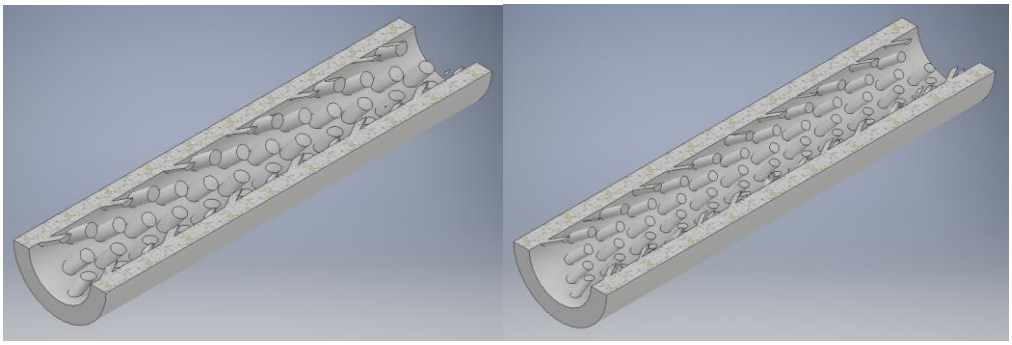

(a) (b)

Figure 1**: CAD models of the pin fin designs A and B, panels (a) and (b), respectively. (shortened and scaled (4:7) for clarity)**

Table 1: Table of AM helical pin fin tube parameters.

	Tube A	**Tube B**	**Conven-tional Tube**	**Conven-tional Welded Tube**	**Finless AM Tube**
Tube ID (mm (inch)) D	7 (0.275)	7 (0.275)	7 (0.275)	7 (0.275)	7 (0.275)
Tube OD (mm (inch))	9.5 (0.374)	9.5 (0.374)	9.5 (0.374)	9.5 (0.374)	9.5 (0.374)
Ellipse Major Diameter (mm (inch)) d	0.749 (0.0295)	0.5 (0.0197)			
Aspect Ratio (Major/Minor)	1	1			
Pin Length (mm (inch))	1.75 (0.0689)	1.75 (0.0689)			
Dimensionless Pin Helical Spacing (s/d)	2	2			
Dimensionless Helix Pitch (p/D)	2	2			
A/A_0	1.8	1.8	1	1	1
Total Length (m (ft))	0.635 (2.08)	0.635 (2.08)	1.52 (5)	0.635 (2.08)	0.635 (2.08)
Segment Length (cm (inch))	12.7 (5)	12.7 (5)		12.7 (5)	12.7 (5)
Welded	Yes	Yes	No	Yes	Yes

SURFACE ROUGHNESS CHARACTERIZATION

In the results section, it is demonstrated that the surface roughness resulting from the additive manufacturing process increases the heat transfer and friction factor yielding a beneficial thermal performance factor. For completeness, the surface roughness of the finless AM tubes considered in these studies was characterized.

Three-dimensional surface roughness profiles were acquired using a white light interferometer (Olympus DSX510). A typical microscope image and surface elevation profile are shown in Figure 2. As visible in the photomicrograph and profile, one important feature of the AM surface

roughness is the presences of sintered particles which have a size which varies from 15 µm to 45 µm. Line roughness parameters (R_a, R_q, R_z) were calculated for each profile, averaged (across 14 samples), and reported in Table 2. Appendix A provides expressions for the roughness parameters and explains their physical significance. The surface roughness characterization procedure was selected following the approach outlined by Stimpson et al. [10].

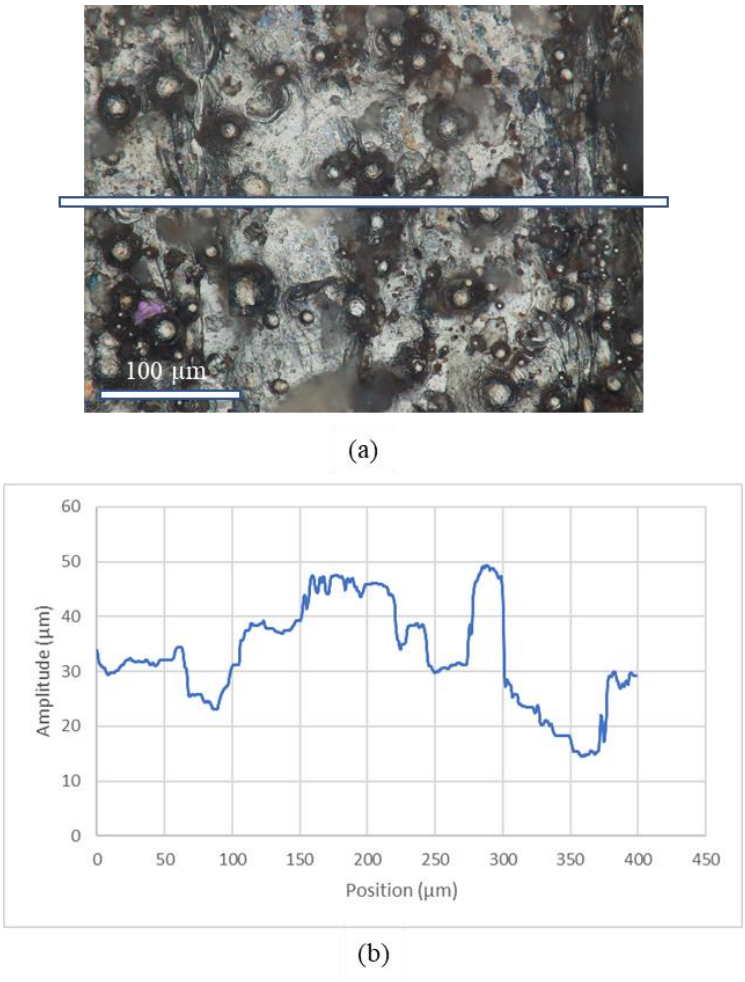

Figure 2: Sample surface roughness: (a) Photomicrograph of additively manufactured surface acquired with a white light interferometer (b) Surface profile acquired along horizontal line drawn on micrograph.

Table 2: Surface roughness parameters for AM manufactured finless tubes ($\bar{\mu} \pm \sigma$)

R_a (µm)	R_q (µm)	R_z (µm)
4.4 ± 1.1	5.5 ± 1.4	21.4 ± 5.7

TEST METHODOLOGY

The test condition selected for this study is the low pressure (LP) outlet in the low temperature recuperator (LTR). In the HEET test facility, this condition was applied to the cold (tube) side inlet. The test temperature, pressure, and Reynolds number range for this test condition are shown in Table 3.

Table 3: Test condition parameters considered in the present study

Location	T (K, (°F))	P (MPa (psia))	Re range of test condition (cold)	Location applied in HEET test facility
LTR, LP Outlet	361 (190)	8.69 (1260)	75k–250k	cold (tube) side

The HEET system was purged and charged with carbon dioxide (while circulating) to the test pressure before acquiring the data. Simultaneously, the system was heated to the test condition temperature. Careful manual control of the syringe pump, heater temperature setpoint, cooling water flow rate, and hot stream and cold stream mass flow rates was required to ensure control points were reached and remained stable. Following a test plan, the cold side flow rate on the tube side was varied while maintaining a constant hot side (shell) mass flow rate and constant average hot side temperature, $(T_{h,in} - T_{h,out})/2$, where $T_{h,in}$ is the hot side inlet temperature and $T_{h,out}$ is the hot side outlet temperature. The average hot side temperature was determined by estimating the hot side inlet temperature necessary to reach the desired operating conditions, heating the hot side inlet to this temperature, and then controlling the heaters to maintain the average hot side temperature of the first test in subsequent tests. Steady state operation was assured by waiting before recording data until the standard deviation in the pressure drop was less than 0.021 kPa (0.003 psi). Although the accuracy of the differential pressure transducer was 0.069 kPa (0.01 psi), 0.021 kPa was selected to assure repeatability between the results.

DATA REDUCTION AND ANALYSIS

The current study relies on the Wilson plot technique applied to a zero-dimensional heat exchanger model to obtain the heat transfer coefficient at the cold (tube) side [4, 7, 8]. In this section the data reduction methodology is briefly presented. The entire methodology is presented in Searle et al. (2020) [9]. The rate of heat transfer (Q) from the hot fluid to a cold fluid in a heat exchanger is

$$Q = U \times A \times LMTD = \frac{LMTD}{R_{ov}} \tag{1}$$

where U is the overall heat transfer coefficient (relative to the tube side area), A is the heat transfer area at the tube side, and $LMTD$ is the log mean temperature difference (measured between the inlets and outlets of the tube and reference side) [11]. $R_{ov} = 1/UA$ is the total resistance between the hot and cold streams. Rearranging Eq (1) yields the overall resistance

$$R_{ov} = \frac{LMTD}{Q} \tag{2}$$

The overall resistance between the hot stream and the cold stream is the sum of convection resistance at the cold side wall (R_c), conduction resistance in the tube wall (R_w), and convection resistance at hot side wall (R_h).

$$R_{ov} = R_c + R_w + R_h \tag{3}$$

The convection resistances are expressed as $R_c = 1/h_c A_c$ and $R_h = 1/h_h A_h$ where h_c is the heat transfer coefficient at the cold side, A_c is the cold side area, h_h is the heat transfer coefficient at the hot side, and A_h is the hot side area. R_c, R_w, and R_h are each unknown. However, R_{ov} can be calculated from experimental temperature measurements utilizing Eq. (2). The experiments are performed so that R_c varies while R_w and R_h remain constant. This is achieved by varying the mass flow rate on the cold side while controlling the mass flow rate and average temperature on the hot side, as stated earlier.

Even though R_c is unknown, one can calculate a cold side resistance value, R_{c0}, with the heat transfer coefficient calculated from the Dittus-Boelter relationship for a heated, fully-developed internal flow.

$$Nu_0 = 0.023 Re_D^{0.8} Pr^{0.4} \tag{4}$$

where $Nu_0 = h_c D/k_f$ will serve as the baseline classical Nusselt number, $Re_D = GD/\mu$ is the Reynolds number based on the tube internal diameter, and Pr is the Prandtl number. Here, h_c is the cold side heat transfer coefficient. k_f is the fluid conductivity. G is the average mass flux. μ is the dynamic viscosity. The fluid properties are estimated at the average temperature and pressure inside the tube using NIST REFPROP [12], and the equation of the state provided in [13]. R_{c0} is calculated with $h_c = h_0$ and $A_c = A_0$

$$R_{c0} = \frac{1}{\mathrm{h}_0 A_0} \tag{5}$$

where A_0 is the smooth (finless) tube area and h_0 is the heat transfer coefficient as calculated with the Dittus-Boelter correlation. Assuming that R_{c0}/R_c is a constant, Eq. (3) can be expressed as

$$R_{ov} = \left(\frac{R_c}{R_{c0}}\right) R_{c0} + R_w + R_h \tag{6}$$

The Wilson plot is now formed by plotting R_{ov} as a function of R_{c0}.

An expression similar to Eq. (5) can be obtained for the finned tube with $h_c = h$ and $A_c = A$, yielding $R_c = D/(Nuk_f A)$. It must be emphasized that h is the heat transfer coefficient in the finned tube with respect to the finned surface area, A.

Taking the ratio of R_c to R_{c0} and rearranging yields:

$$\frac{Nu}{Nu_0} = \frac{\mathrm{R_{c0}}}{R_c}\frac{A_0}{A} \tag{7}$$

Thus, the Nusselt number ratio may be determined with the Wilson plot line slope (R_c/R_{c0}) and the ratio of A to A_0.

An experimental study of a heat exchanger is incomplete without reporting the pressure drop of the heat exchanger. The tube-side pressure drop is reported in terms of its friction factor

$$f = \frac{\pi^2}{8}\frac{\Delta P\ \rho\ D^5}{L\ \dot{m}^2} \tag{8}$$

where ΔP is the pressure drop across the tube, L is the length of the tube, D is the tube inner diameter, ρ is the density of the fluid in the tube evaluated at the average temperature and pressure, and $\dot{m}$ is the mass flow rate in the tube [14].

A reference friction factor for turbulent flow in a smooth tube is calculated using the McAdams correlation

$$f_0 = 0.184 Re_D^{-0.2} \tag{9}$$

which is valid for 30k < Re_D < 2000k [2]. This value is utilized to estimate f/f_0.

RESULTS AND DISCUSSION

The first set of results to be discussed is a typical Wilson plot and a corresponding plot of pressure drop per unit length. This will be followed by a discussion on the heat transfer enhancement (increase in heat duty). Finally, the corresponding increase in friction factor is reported and discussed.

Wilson Plot

The Wilson plot, as introduced in the analysis section, is a graphical method of determining the heat transfer coefficient on either the hot or cold side of a heat exchanger. In this scenario, the cold side (tube side) of a single pass shell and tube heat exchanger is considered. The Wilson plot is constructed by plotting the measured total heat transfer resistance, R_{ov}, as a function of the local resistance, R_c, as calculated by the Dittus-Boelter correlation. Lines may be fit to each data set, where the slope is the ratio, $h_0 A_0/hA$, and the intercept is $R_h + R_w$. A slope of 1 indicates that the experimental data agrees exactly with the value predicted by the Dittus-Boelter correlation.

A Wilson plot is displayed in Figure 3 for results obtained at test condition 1. Results for the conventional tube, the finless AM tube, and tube designs A and B are shown. A linear fit to the conventional tube data shows that the Dittus-Boelter correlation predicts the tube side resistance within 4% over Re_D ranging from 79k to 246k.

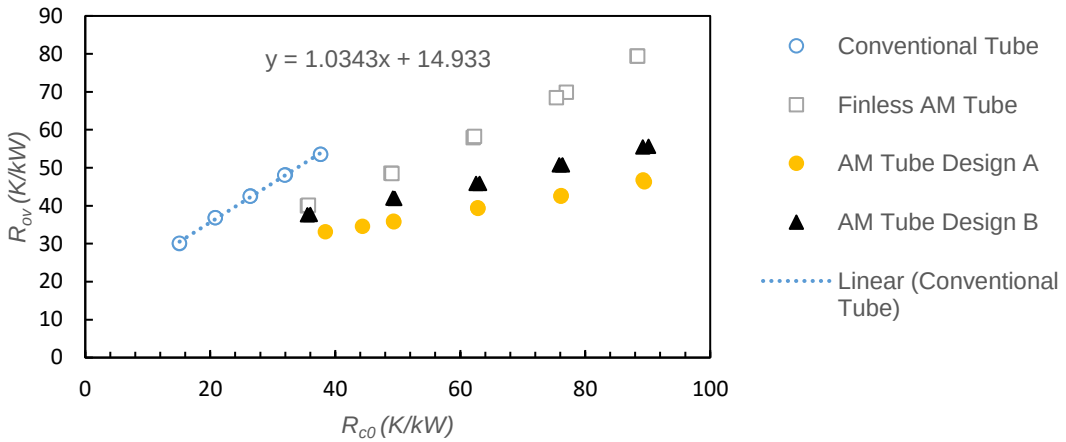

Figure 3: Typical Wilson plot ($79\mathbf{k} < Re_D < 246\mathbf{k}$)

In Figure 4, pressure drop per unit length (kPa/mm) is shown at different Re_D for each tube design considered in this study. The AM tube designs, A and B, have an order of magnitude larger pressure drop per unit length.

It can be observed that the conventional welded tube has a lower pressure drop per unit length than the conventional tube and this can be attributed to an anomalous 68.9 kPa (10 psi) variation in the average tube inlet pressure during these tests.

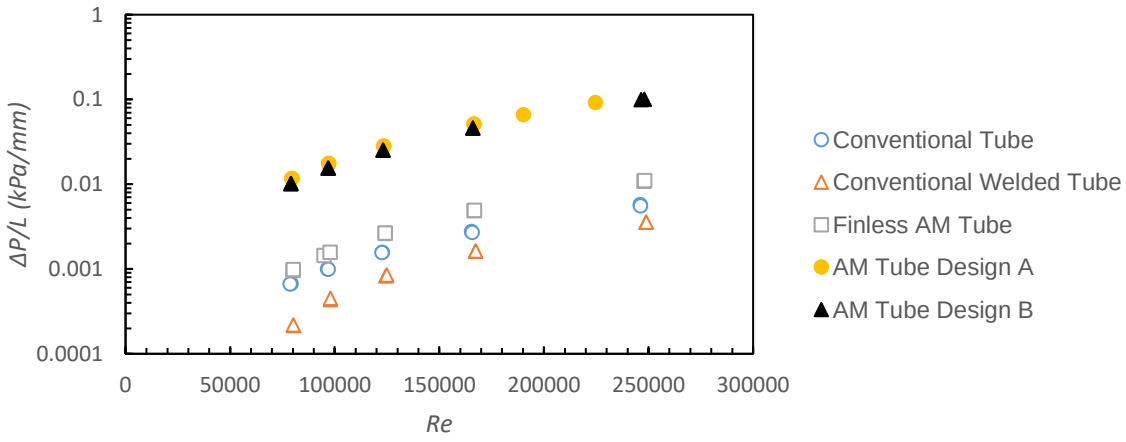

Figure 4: Pressure drop per unit length (*ΔP/L*) for varying Re_D

Heat Transfer Enhancement

The heat transfer enhancement, hA/h_0A_0, is plotted in Figure 5 panel (a) for each tube design listed on the horizontal axis. hA/h_0A_0 represents the increase in heat transfer per unit log mean temperature difference in the finned tubes relative to the heat transfer in the smooth tube, where h is calculated with the Dittus-Boelter correlation. For the finned tubes, hA/h_0A_0 increases by 282% and 204%, for tube designs A and B, respectively. As a final observation, the finless AM

tube experiences a greater heat transfer rate than the conventional tube (27%) but less than the finned designs. This can be attributed to the surface roughness. It must be noted that the analysis estimates the surface area of the rough AM tube to be same as that of the smooth tube.

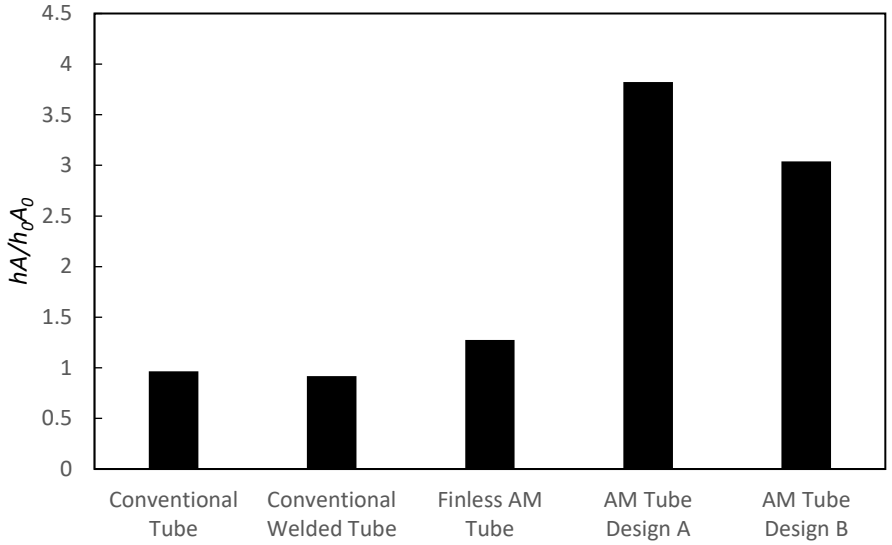

(a)

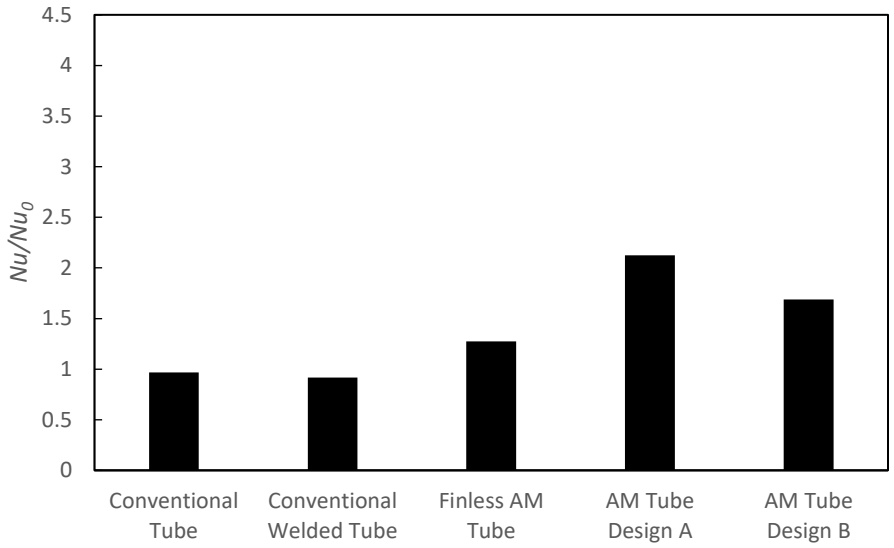

(b)

Figure 5: (a) Heat transfer enhancement, hA/h_0A_0 (b) Nu/Nu_0 ratio

hA/h_0A_0 increases due to the increase in both the heat transfer coefficient as well as the heat transfer area. To differentiate between the increase due to the heat transfer coefficient and the increase due to the surface area, $Nu/Nu_0 = h/h_0$ is plotted in Figure 5 panel (b). The Nusselt

number ratio is valuable because it represents how much advection has increased through the addition of the pin fins. It must be kept in mind that Nu/Nu_0 is equal to hA/h_0A_0 for the conventional tube, the conventional welded tube, and the finless AM tube. As listed in Table 1, the area ratios for tube design A and B are 1.8. Dividing by the area ratios yields values for Nu/Nu_0 (panel (b)) that are less than values for hA/h_0A_0 (panel (a)). The tubes rank in order of increasing heat transfer coefficient: tube B and tube A, with corresponding percent increase in the heat transfer coefficient relative to the Dittus-Boelter correlation of 69%, and 112%.

Friction Factor

While the increase in hA/h_0A_0 and Nu/Nu_0 shown in the previous section is encouraging, this enhancement must be weighted by the increase in the friction factor when considering the thermal performance of the tube designs. Shown in Figure 6 are the results for f/f_0. The friction factors for the conventional tube agree within 3% with the McAdams correlation and the friction factors for the conventional *welded* tube agree within 8% with the McAdams correlation. While the finless AM tube has a friction factor 134% larger than the McAdams correlation, the tube designs have friction factor an order of magnitude larger than the smooth tube correlation (nominally 2300%).

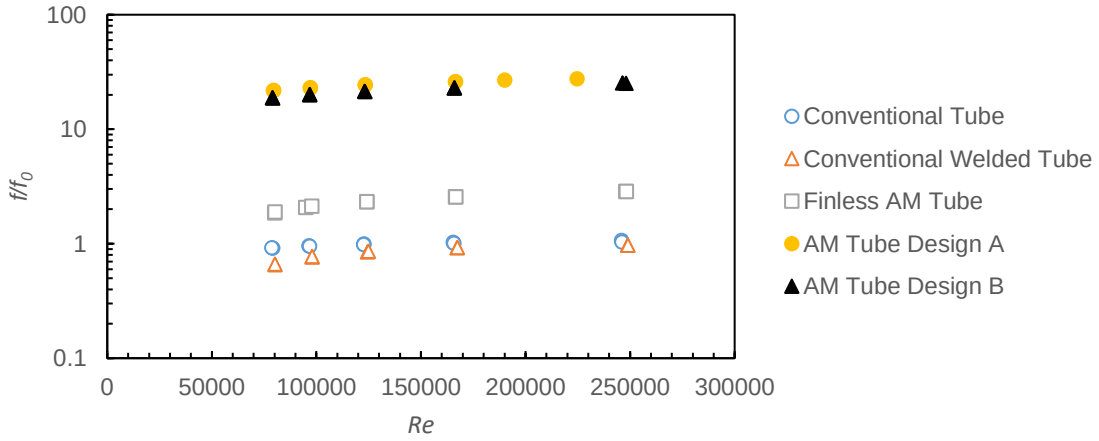

Figure 6: Friction factor ratio for varying Re_D.

Companion Study and Future Work

A companion study at NETL has sought to reduce the volume of pin fin designs by utilizing CFD to determine Nu/Nu_0 and f/f_0 of candidate pin fin tubes. The results of the present experimental study were utilized as a validation for the CFD simulation with $(Nu/Nu_0)/(f/f_0)^{1/3}$ agreeing within 10%.

Several high performing candidate designs from this optimization study will be fabricated at the Oak Ridge National Lab and tested at the National Energy Technology Laboratory in Morgantown, WV. The results of these experiments will be utilized to estimate how much heat exchanger material can be reduced by using high performing pin finned tube designs.

CONCLUSIONS

This work reports experiments performed in the Heat Exchange and Experimental Testing (HEET) facility at the U.S. DoE's National Energy Technology Laboratory. The Wilson plot technique was utilized to measure the heat transfer coefficients in supercritical carbon dioxide flowing through additively manufactured tubing with pin fins. The following conclusions were made:

- The results for a smooth, conventional tube agreed within 5% of the Dittus-Boelter correlation for heat transfer and within 7% of the McAdams correlation for pressure drop, validating the HEET measurements
- For the best performing helical pin fin design, the tube side conductance increased by 282% and the heat transfer coefficient increased by 112% relative to the Dittus-Boelter correlation.
- Across the range of Re_D considered (7×10^4 to 2.5×10^5), the average friction factor increased by 2300% relative to the McAdams correlation.

ACKNOWLEDGEMENTS

The authors wish to acknowledge the contributions of Dennis Lynch, Mike Ciocco, Curtis Batton, Mark Tucker, Jeff Riley, and Rich Eddie for their meticulous efforts in reviewing and modifying the design, constructing the test rig, designing the instrumentation and control system, developing the test procedure, and collecting experimental data.

This work was supported in part by an appointment to the U.S. Department of Energy (DOE) Postgraduate Research Program at the National Energy Technology Laboratory (NETL). This appointment was administered by the Oak Ridge Institute for Science and Education (ORISE).

APPENDIX A: SURFACE ROUGHNESS PARAMETERS

Surface roughness characterization of additively manufactured surfaces was well-defined in a paper by Stimpson et al. [10]. Arithmetic mean roughness, R_a, root-mean-square roughness, R_q,

mean roughness depth, R_z, were defined. The expressions for these roughness parameters are repeated here and their significance explained.

$$R_a = \frac{1}{n}\sum_{i=1}^{n} |z_i - \mu| \tag{A.1}$$

$$R_q = \sqrt{\frac{1}{n}\sum_{i=1}^{n} (z_i - \mu)^2} \tag{A.2}$$

$$R_z = \frac{1}{n}\sum_{i=1}^{n} (z_{max} - z_{min})_i \tag{A.3}$$

where z_i are profile heights along a surface roughness profile, μ is the mean height, z_{min} is the minimum height, z_{max} is the maximum height, and n is the number of points along the profile.

R_a is the arithmetic average roughness and is a measure of the average variation of the roughness profile about the mean. R_q is the root-mean-square roughness and is a measure of the variation of the roughness profile about the mean but unlike the arithmetic roughness weights larger variations more than smaller variations. R_z is the mean roughness depth and can be defined in different ways. Here it is defined as the average of the maximum minus the minimum height for five different regions along the profile.

REFERENCES

1. Bush, V., *GTI STEP forward on sCO2 Power*, in *6th Int. sCO2 Power Cycle Symposium*. Pittsburgh, PA.
2. White, C.W., et al., *sCO2 Cycle as an Efficiency Improvement Opportunity for Air-fired Coal Combustion*, in *6th Int. sCO2 Power Cycle Symposium*. 2018: Pittsburgh, PA.
3. White, C.W. and N.T. Weiland, *Preliminary Cost and Performance Results for a Natural Gas-fired Direct sCO2 Power Plant*, in *6th Int. sCO2 Power Cycle Symposium*. Pittsburgh, PA.
4. Black, J., et al., *Measurement of Convective Heat Transfer Coefficients with Supercritical CO2 using the Wilson-Plot Technique*, in *The 44th International Technical Conference on Clean Energy*. Clearwater, Florida, USA.
5. Musgrove, G., M. Portnoff, and S. Sullivan, *Heat Exchangers for Supercritical CO2 Power Cycle Applications*.
6. Wilson, E.E., *A Basis for Rational Design of Heat Transfer Apparatus.* Transactions of ASME, 1915. **37**.
7. Briggs, D.E. and E.H. Young, *Modified Wilson-Plot Techniques for Obtaining Heat Transfer Correlations for Shell and Tube Heat Exchangers.* Chem. Eng. Prog. Sym. Ser. , (No. 22, 65): p. 35-45.

8. Fernández-Seara, J., et al., *A general review of the Wilson plot method and its modifications to determine convection coefficients in heat exchange devices.* Applied Thermal Engineering, 2007. **27**(17-18): p. 2745-2757.

9. Searle, M., et al., *Measurement of Convective Heat Transfer Coefficients with Supercritical CO2 in Novel Additively Manufactured Helically Patterned Pin Fin Tubes Using the Wilson Plot Technique.* 2020: Manuscript prepared for submission to *Applied Thermal Engineering*.

10. Stimpson, C.K., et al., *Scaling Roughness Effects on Pressure Loss and Heat Transfer of Additively Manufactured Channels.* Journal of Turbomachinery, 2016. **139**(2): 021003.

11. Incropera, F.P., et al., *Fundamentals of Heat and Mass Transfer*. 6 ed. 2006: John Wiley & Sons.

12. Lemmon, E.W., et al., *NIST Standard Reference Database 23: Reference Fluid Thermodynamic and Transport Properties-REFPROP*. 2018, National Institute of Standards and Technology: Gaithersburg.

13. Span, R. and W. Wagner, *A New Equation of State for Carbon Dioxide Covering the Fluid Region from the Triple-Point Temperature to 1100 K at Pressures up to 800 MPa.* Journal of Physical and Chemical Reference Data, 1996. **25**(6): p. 1509-1596.

14. Munson, B.R., et al., *Fundamentals of Fluid Mechanics*. 6 ed. 2009: John Wiley & Sons, Inc.

AUTHORS

Dr. Matthew Searle received his PhD in Mechanical Engineering from Brigham Young University in December 2018. He is an Oak Ridge Institute for Science and Engineering (ORISE) Postdoctoral Researcher at the U.S. Department of Energy's National Energy Technology Laboratory (NETL). Matthew's areas of expertise are experimental and analytical thermal science. He is interested in applying experimental heat transfer research to improve energy conversion efficiency in thermal power cycles.

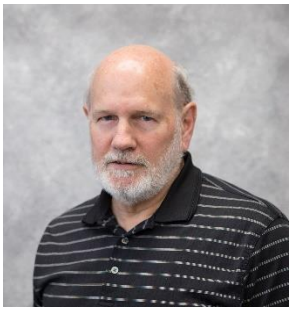

Dr. Jim Black is an Engineer in the Research and Innovation Center (RIC) at NETL working on Aerothermal and Heat Transfer research. In this position he conducts research on turbines thermal management and heat transfer for gas and supercritical CO_2 turbine. Prior to moving to RIC, Dr. Black performed techno-economic analyses of advanced fossil energy conversion processes. He has more than 35 years of experience including positions as project manager of a DOE funded demonstration of a combined SOx/NOx removal technology, research engineer at Gulf Research studying oil production of heavy oils using steam stimulation, and test engineer during the startup of Beaver Valley Unit 1 nuclear power plant. Dr. Black earned B.S., M.S., and Ph.D. degrees in Mechanical Engineering from the University of Pittsburgh and holds a Professional Engineering license in Pennsylvania.

Doug Straub is a Research Engineer at the U.S. Department of Energy's National Energy Technology Laboratory, and has over 25 years of experience in the fields of experimental combustion and heat transfer. Doug's publications and patents have been widely cited and cover a diverse range of topic areas. Doug has been instrumental in developing several unique experimental capabilities at NETL, including the high-pressure CO_2 flow loop to measure average heat transfer coefficients and pressure drop at 200 bar.

Edward H Robey, Jr. received his MS Degree in Statistics from West Virginia University in 1985. He is currently the activity manager for the Aerothermal Project with the Leidos Research Support Team (LRST) working as an on-site contractor to the National Energy Technology Laboratory (NETL) in Morgantown, WV.

Edward's contributions at NETL (formerly the Morgantown Energy Technology Center and the Federal Energy Technology Center) have involved statistical analysis of natural gas extraction and gas reservoir modeling data to identify production trends associated with fracture zones in tight Devonian shale formations. Edward has supported analysis in the technical areas of unsteady combustion, fluidization, combustion of coal-water slurry, and diesel operation on coal-derived fuels.

Under Parsons as the site support contractor, Edward worked on a variety of fuel-cell projects including testing of prototype power units for the Solid-state Energy Conversion Alliance (SECA) program and the first demonstration of solid oxide fuel cell operation on reformed biodiesel.

More recently, under LRST, he has been performing infra-red image analysis related to turbine blade cooling experiments. This has lead to a collaboration with other NETL researchers in analysis of aerothermal cooling measurements in NETL's high-temperature, high-pressure, thermally conductive environment and resolving differences between NETL's results and those see in ambient-temperature, ambient-pressure, adiabatic systems.

Dr. M. Joseph Yip is a Mechanical Engineer performing research in combustion systems in NETL, U.S. DoE since 1991. Prior to joining NETL, M. Joseph also worked in nuclear power plant certification industry. M. Joseph started his engineering career in NETL as an experimentalist in combustion stability in combustors, and later into optical measurement in combustion projects. M. Joseph received his doctoral degree in Mechanical Engineering from the Ohio State University, Columbus, OH.

Dr. Sridharan Ramesh received his Ph.D. from Virginia Tech in 2016. He is a currently working at LRST as a Research Engineer/site support contractor to the National Energy Technology Laboratory (NETL) in Morgantown, WV. Sridharan has been involved in the field of gas turbine heat transfer for about 6 yrs. His background includes experience in experimental heat transfer, conjugate CFD and radiation modeling, gas turbine heat transfer, thermal management, heat exchangers and supercritical carbon-dioxide heat transfer and power cycles.

Dr. Arnab Roy currently works as a Research Scientist/Engineer at the National Energy Technology Laboratory, Morgantown, as a part of Leidos Research Support Team (LRST), contractor to the US Dept. of Energy. He received his Bachelors from Jadavpur University, India in 2007, Masters from University of Connecticut in 2010 and PhD from Virginia Tech in 2014, all in Mechanical Engineering. After graduating from Virginia Tech with a PhD working on experimental methods in gas turbine endwall heat transfer and cooling technology, he joined NETL in 2014. Since joining NETL, he has been primarily working on the "Pressure Gain Combustion for Land Based Power Generation" research project, while also supporting other projects on supercritical CO_2 technology and turbine thermal management within the Thermal Sciences team at the NETL Research and Innovation Center. Dr. Roy as authored/co-authored several publications in journals and conferences on diverse research areas such as pressure gain combustion, gas turbine heat transfer and cooling, sCO2 heat transfer, Polymer Electrolyte Fuel Cells and Coal Gasification.

Dr. Adrian Sabau is a Computational Materials Scientist in the Computational Sciences & Engineering Division of ORNL. Dr. Sabau received an Engineer Diploma from the University of Craiova, Romania and a PhD degree in Mechanical Engineering from Southern Methodist University in 1996. Dr. Sabau seeks to advance materials processing, laser processing, and materials for energy applications through the development of computational and experimental techniques for property measurements, process analysis, and in-service materials behavior. Dr. Sabau is an ASME fellow and the recipient of three R&D 100 awards in process sciences and published more than 140 technical papers

Dr. Fred List is a Senior Research Scientist at Oak Ridge National Laboratory in the Materials Science & Technology Division at the Manufacturing Demonstration Facility. For nearly the past decade, he has been involved with designing, manufacturing, and testing of additive metal components including geothermal heat exchangers, neurosurgical aneurysm clips, compact nuclear reactors, and injection molding tooling. While at ORNL he has also contributed to the development of high temperature superconductors for commercial applications. He earned a B.S. in Applied and Engineering Physics and a Ph.D. in Materials Science/Physics from Cornell University

Keith Carver is a Technician/Engineer working with laser powder bed additive metals at ORNL/MDF. Scope of work includes design of experiments, parts design/redesign for additive processes, machine programming/operation/maintenance, and assisting with in-situ data collection.

Dr. Darren Mollot is the Director of Exploratory Research and Innovation in the Office of Fossil Energy at the U.S. Department of Energy (DOE). In this position, Dr. Mollot advices senior management on scientific and technological breakthroughs, directs exploratory research projects designed to rapidly accelerate high risk, high programmatic impact research, and identify potential opportunities to accelerate progress toward Office objectives.

He has worked for the DOE's Office of Fossil Energy since 1992 and has served in many roles including most recently as Associate Deputy Assistant Secretary for Clean Coal and Carbon Management in the Office of Fossil. Dr. Mollot has also served as Office Director for Advanced Fossil Technology Systems, as a Research Scientist and Project Manager at the National Energy Technology Laboratory, Technical Liaison and start-up Team Lead at the National Carbon Capture Center, as the turbines Program Manager. In 1999, Dr. Mollot was selected as a Congressional Science Fellow and served for a year under Senator Rockefeller.

Prior to joining DOE, Dr. Mollot worked in the private sector, holding positions with IBM and Westinghouse Electric Corporation. He earned his Doctor of Philosophy from the State University of New York at Buffalo in Mechanical and Aerospace Engineering.